

# A combined QEXAFS/XRD method for on-line, in situ studies of catalysts: examples of dynamic measurements of Cu-based methanol catalysts

Bjerne S. Clausen, Lars Gråbæk, Gert Steffensen, Poul L. Hansen  
and Henrik Topsøe

*Haldor Topsøe Research Laboratories, DK-2800 Lyngby, Denmark*

The development of a new in situ method which allows high quality XRD and EXAFS to be obtained on-line under ideal catalytic conditions is discussed. The possibility to obtain both types of information simultaneously enables a much better structural description of catalytic materials which typically contain both crystalline and X-ray amorphous structures. The system employs a capillary tube as the microreactor/in situ cell. The high degree of temperature uniformity of the cell and the possibilities of fast changes in reaction conditions make the system ideal for dynamic studies. For this purpose, the EXAFS measurements are carried out in the newly developed quick scanning mode (QEXAFS) which also allows high quality data to be obtained. The XRD is acquired using a position sensitive detector. The application of the setup for time resolved measurements is demonstrated in a study of the calcination and reduction of Cu-based methanol catalysts where the changes take place over a few degrees. The high quality of the data made it possible to obtain important new insight regarding the presence of intermediate phases during these processes. Studies of Cu/SiO<sub>2</sub> catalysts show the advantages of a newly developed theory for a better estimation of coordination numbers (and thus particle sizes) from EXAFS.

**Keywords:** EXAFS; QEXAFS; XRD; methanol catalyst; molecular dynamics; in situ studies; Cu catalysts

## 1. Introduction

For many years, X-ray diffraction (XRD) has been the most commonly applied method to study the well-ordered or crystalline part of catalyst structures. In recent years, it has been shown that extended X-ray absorption fine structure (EXAFS) can be used to provide information on the amorphous and micro-crystalline structures in heterogeneous catalysts (see, e.g., ref. [1]). It is evident that XRD and EXAFS compliment each other. An ideal structural technique is thus one where the two types of measurements are carried out simultaneously. This would lead to a much improved structural description of catalysts which often contain both crystalline and X-ray amorphous structures. Moreover, both techniques

have the ability for providing the information in situ, while the catalysis takes place. However, in spite of the possibilities, the above-mentioned potential has not been fully exploited. For example, the XRD and EXAFS experiments are not always carried out under realistic in situ conditions. Also the two techniques are normally used with widely different sample sizes and sample geometries and thus the studies have traditionally been carried out in separate experimental setups. This makes, of course, a common interpretation of the results uncertain since catalyst structures are very dynamic and even small differences in experimental conditions may result in different catalyst structures. To avoid these complexities, it is of course especially important to carry out the different studies simultaneously under the realistic reaction conditions. This would also allow one to directly establish structure–activity relationships.

Recently, we have shown that glass or quartz capillaries may be used as combined XRD cells and catalytic microreactors [2]. The cells allowed good quality XRD data. However, equally important is the fact that the cells offer ideal conditions for catalysts (plug flow, elimination of temperature gradients, etc.) such that realistic catalytic and structural information can be obtained simultaneously on the same sample. In addition, the cells are capable of operating both at high temperatures and high pressures and allow rapid changes in conditions such that dynamic studies can be performed. In the present work, we will show that the capillary microreactors may also serve as in situ cells in EXAFS experiments. Moreover, the goal of a combined technique has been met since both types of measurements can be performed in a newly constructed combined EXAFS/XRD setup. A preliminary account of the setup and its use were given in ref. [3]. The present paper describes in detail the combined EXAFS/XRD method and its use in dynamic in situ studies. Recently, Thomas and coworkers [4,5] have also been active in developing a combined EXAFS and XRD method and have shown that time resolved studies can be performed using EXAFS in the energy dispersive mode (DEXAFS). However, it is in general much more difficult to obtain reliable high quality EXAFS spectra with the DEXAFS technique than with EXAFS in the normal energy scanning mode due to the requirements of extreme sample uniformity to avoid additional background oscillations interfering with the EXAFS. Furthermore, non-linearity in the energy scale may complicate the analysis. In view of the recent promising developments of EXAFS in the quick scanning mode (QEXAFS) [6], which does not have the above drawbacks, it appears more advantageous to use this technique for time resolved studies. In the present work, we have thus extended our previous time resolved studies by implementation of the QEXAFS technique and at the same time we have taken advantage of the capabilities of the capillary microreactor/in situ cell [2] and the combined XRD/EXAFS setup. This has allowed studies of rapid phase transformations and has given new insight into the calcination and reduction processes of Cu-based methanol catalysts.

Finally, it is shown how the combined XRD and EXAFS information from the

new technique has been crucial in confirming the advantages of a new procedure for obtaining a better estimation of the size of small metallic particles from EXAFS [7,8].

## 2. Combined XRD/EXAFS setup

The combined EXAFS/XRD measurements in transmission can be performed on the same sample by mounting a diffractometer between the first and the second ionization chamber in a standard EXAFS spectrometer setup. The diffractometer is of the Debye–Scherrer type with the capillary microreactor mounted horizontally and the diffracted X-rays are detected in the vertical plane. A schematic drawing of the setup is shown in fig. 1.

The design of the combined capillary microreactor/in situ cell has been described in detail in ref. [2]. In short, the cell consists of a capillary tube made of quartz connected to stainless steel in- and outlet tubes via standard Swagelok tube fittings. The outer diameter of the capillary is typically 0.5 mm and the wall thickness 0.01 mm. The capillary reactor is heated by passing a stream of hot gas ( $N_2$ ) over it. Temperature homogeneity is ensured by enclosing the capillary reactor in a Kapton heat shield.

In order to record EXAFS without spurious oscillations, the sample thickness over the beam area must be relatively uniform. This is ensured of the capillary

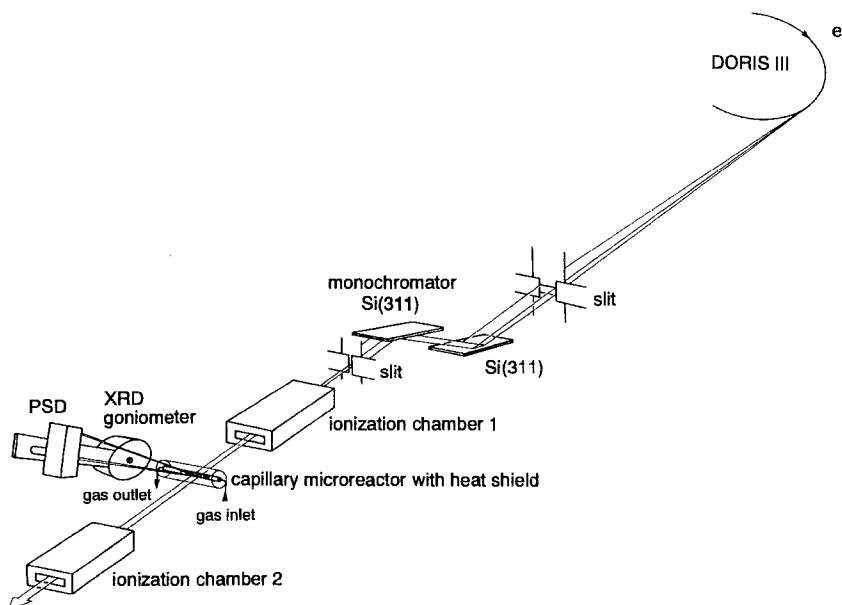


Fig. 1. Schematic drawing of the setup which allows combined QEXAFS/XRD in situ studies and simultaneous catalytic measurements.

microreactor by defining the beam by narrow slits with a vertical opening of only 0.2 mm.

The setup can be operated in two different ways. For high resolution, high quality data, the EXAFS is recorded by step scanning the monochromator through the energy region of interest. The X-ray diffractograms are then collected during an EXAFS scan simply by stopping the monochromator scan at a suitable wavelength for the time needed to collect the data and then continuing with the EXAFS scan. This mode was used in the present study to experimentally verify the advantages of the novel EXAFS analysis procedure for small particles [7,8]. For improved time resolved studies, the quick scanning EXAFS technique (QEXAFS) in which the monochromator is continuously scanned through the energy region was employed. To minimize the recording time for the XRD pattern, a position sensitive detector (PSD) was used. The sample–detector distance and the detector length determine the resolution and the angular range of the data collected in one diagram. A full diagram can of course be constructed by splining several diagrams obtained at different  $2\theta$  regions or alternatively by use of a wide angle PSD as employed in ref. [5].

### 3. Experimental

The XRD/EXAFS experiments were performed at HASYLAB at DESY (Hamburg, Germany) using the synchrotron radiation from the DORIS III storage ring. Two parallel Si(311) crystals were used to monochromatize the X-rays. The content of higher harmonics in the monochromatized beam was minimized by slightly detuning the crystals from parallel. The intensity of the incident and transmitted X-rays was recorded by use of  $N_2$ -filled ionization chambers. In order to achieve an accurate energy calibration of the EXAFS spectra, data of the catalyst and a reference sample ( $Yb_2O_3$ ), inserted between the second and a third ionization chamber, were measured simultaneously. For the XRD, a wave length of 0.14 nm was chosen to prevent fluorescence from the copper in the sample. The diffracted X-rays were detected by use of an Ar- $CH_4$  gas filled position sensitive wire detector (MBraun GmbH) with a resolution of 50  $\mu m$ . From measurements of highly crystalline  $SiO_2$ , it was found that the angular resolution is essentially given by the diameter of the capillary tube and the distance from the sample to the detector. In the present study, the detector covered a  $2\theta$  angle of about  $7^\circ$  and the resolution was typically  $\Delta 2\theta = 0.05^\circ$ .

For the time resolved studies, a binary Cu/ZnO catalyst with a Cu/(Cu + Zn) ratio of 0.50 and a ternary Cu/ZnO/ $Al_2O_3$  catalyst with a Cu/(Cu + Zn) ratio of 0.30 were investigated. These catalysts were prepared by coprecipitation from the metal nitrates as described in detail in ref. [9]. The silica supported Cu catalysts, which were used for verifying the improved EXAFS analysis for small parti-

cles, were prepared as described in ref. [7] following the procedure of Geus and co-workers [10].

The optimum absorber thickness of about 1.5 absorption lengths was achieved by mixing the catalysts with appropriate amounts of graphite. About 2–4 mg of catalyst sample was loaded in the capillary microreactor and subjected to a flow of the reaction gas. Calcination was carried out in a flow of dry air, whereas the reduction was performed in a flow of argon containing 0.5% CO, 4% CO<sub>2</sub> and 4% H<sub>2</sub> at ambient pressure. The Cu/SiO<sub>2</sub> samples were studied *in situ* after reduction at 493 K. The binary Cu/ZnO and the ternary Cu/Zn/Al<sub>2</sub>O<sub>3</sub> catalysts were studied in the time resolved fashion during the calcination and the reduction process, while slowly increasing the temperature up to the final reaction temperature (673 K). A set of XRD and QEXAFS measurements was obtained every 5 min. The XRD diagram was recorded in 90 s, whereas the subsequent QEXAFS was recorded in 120 s. About 90 s was used to move the monochromator back to the starting energy (8800 eV) where the XRD patterns were recorded (since the XRD data were acquired using a high number of channels, and averaging procedure has been applied for purposes of improved signal/noise). Depending on the region to be scanned, the statistics desired, and the brilliance of the storage ring, faster scans are of course possible.

## 4. Results and discussion

### 4.1. TIME RESOLVED IN SITU STUDIES OF CATALYSTS

Dynamic *in situ* studies of Cu-based methanol catalysts will presently be discussed and used to demonstrate the capabilities of the combined QEXAFS/XRD method.

Industrial Cu/ZnO/Al<sub>2</sub>O<sub>3</sub> methanol catalysts are structurally rather complex. The catalysts have been subject to numerous investigations but the structure of the active surface, the nature of the active sites, and the reaction mechanism are still subject to considerable controversy (see, e.g., refs. [11–13]). Previous studies of different Cu catalysts by XRD, EXAFS and XANES all show that in the active catalysts, the principal Cu component is metallic copper [2,4,14–20].

In order to obtain further information on the processes taking place during calcination and activation of both binary Cu/ZnO and ternary Cu/ZnO/Al<sub>2</sub>O<sub>3</sub> catalysts, we have performed on-line time resolved studies with the combined XRD/QEXAFS technique described in the present work. The changes taking place during calcination will be discussed for the binary catalyst with a Cu/(Cu+Zn) ratio of 0.50 (figs. 2 and 3), whereas the reduction process will be discussed for the ternary catalyst with a Cu/(Cu+Zn) ratio of 0.30 (figs. 4–6).

One of the most important features of the present combined QEXAFS/XRD technique is the ability to obtain high quality EXAFS and XRD data. Figs. 2 and 4

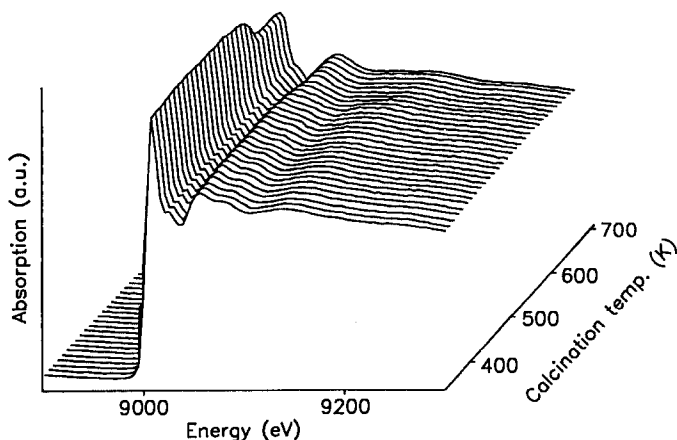


Fig. 2. Raw in situ QEXAFS data near the Cu K-edge obtained on-line during the calcination of the Cu/ZnO catalyst with  $\text{Cu}/(\text{Cu} + \text{Zn}) = 0.50$ .

show that the QEXAFS technique provides excellent EXAFS spectra with no spurious oscillations in the background. Thus, the results show that by use of QEXAFS one can overcome some of the problems encountered when using DEXAFS [4] where the presence of artifacts in the spectra makes a quantitative analysis of such results difficult.

Another and equally important feature of the combined method is the ability to combine realistic catalytic information with structural insight. The features of the catalytic microreactor are discussed in ref. [2]. In both kinetic studies and dynamic studies of changes in catalyst structure, fast temperature responses and the avoidance of temperature and concentration gradients are important. The present setup appears to be ideal in these respects since phase changes occurring over an extremely narrow temperature range (see, e.g., fig. 6) can easily be followed.

The QEXAFS spectra measured during the calcination process of the binary catalyst are shown in fig. 2 as raw data. Although a full data set (8800–9700 eV) has

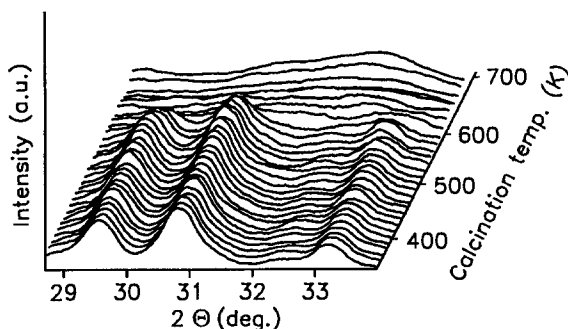


Fig. 3. In situ XRD data obtained on-line during the calcination of the Cu/ZnO catalyst with  $\text{Cu}/(\text{Cu} + \text{Zn}) = 0.50$  (recorded simultaneously with the QEXAFS data in fig. 2).

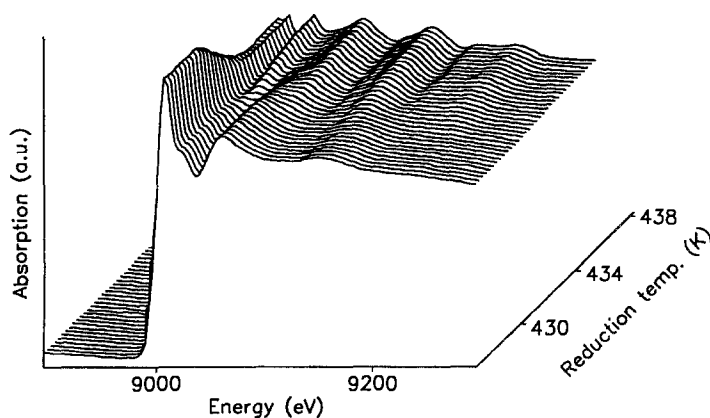


Fig. 4. Raw in situ QEXAFS data near the Cu K-edge obtained on-line during the reduction of the Cu/ZnO/Al<sub>2</sub>O<sub>3</sub> catalyst with Cu/(Cu + Zn) = 0.30.

been recorded for each spectrum, only 400 eV around the edge is shown for better visualizing the changes occurring. In a narrow temperature region around 600 K, a reduction in intensity of the white line as well as a coalescence of the double peak feature into one broad peak in the XANES region near 9070 eV are observed. Clearly, EXAFS can provide insight into the very large changes in the local environments of the Cu atoms occurring during calcination. The spectrum at the highest calcination temperature is indicative of the presence of CuO. The simultaneously recorded XRD diffractograms in the  $2\theta$  angular region, where the strongest CuO line is expected, are shown in fig. 3. Diffractograms of the catalyst before calcination show diffraction lines typical of the auricalcite phase. During calcination, this phase is found to transform into poorly crystalline ZnO- and CuO-like phases in the same temperature range where the QEXAFS is found to change significantly. A close inspection of the XRD data indicates that weak diffraction

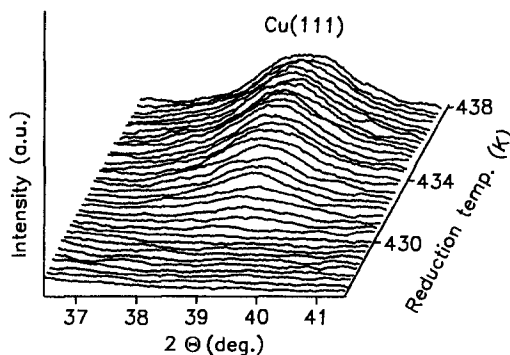


Fig. 5. In situ XRD diffractograms of the Cu(111) line obtained on-line during the reduction of the Cu/ZnO/Al<sub>2</sub>O<sub>3</sub> catalyst with Cu/(Cu + Zn) = 0.30 (recorded simultaneously with the QEXAFS data in fig. 4).

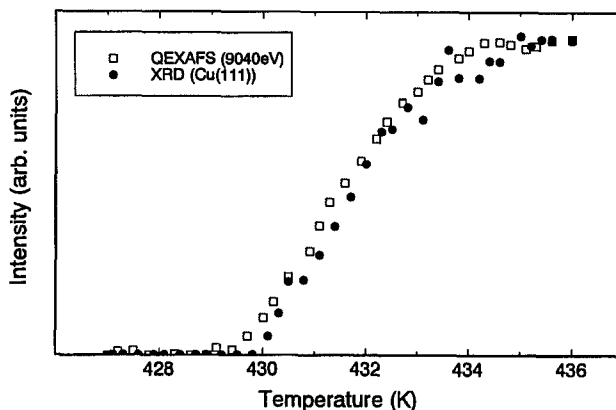


Fig. 6. Changes in the X-ray absorption at 9040 eV during reduction of the Cu/ZnO/Al<sub>2</sub>O<sub>3</sub> catalyst (open squares). Changes in the integrated intensity of the Cu(111) XRD line during reduction (closed circles). The intensities have been scaled to coincide at low and at high temperatures.

lines appear and disappear in this temperature range indicating the presence of intermediate phases during decomposition of the auricalcite phase.

A 3D plot of the raw QEXAFS data for the ternary catalyst recorded *in situ* during reduction is shown in fig. 4. For reasons of clarity, only spectra in the temperature range where the reduction takes place are shown. Upon increasing the reduction temperature, the spectra typical of CuO are observed to change into spectra typical of metallic Cu. This is most clearly observed in the appearance of a pre-peak at half maximum of the absorption edge and the splitting of the white line. Note that the phase transformation from the CuO-like phase to metallic Cu takes place within a few kelvin. In fig. 5, the simultaneously recorded XRD diagrams are shown for the  $2\theta$  angular region where the Cu(111) peak appears.

The changes occurring in the narrow temperature region can be followed in more detail by plotting the intensity of a specific feature in the X-ray absorption spectra as a function of the reduction temperature. This has been done for the feature at 9040 eV which shows a deep valley at low temperature but an intense peak at high reduction temperature (open squares in fig. 6). The integrated intensity of the Cu(III) peak as a function of the reduction temperature is also shown in fig. 6 (closed circles). A comparison of the XRD and the QEXAFS intensity data in fig. 6 reveals that Cu metal appears in the QEXAFS at a slightly lower temperature than in the XRD results indicating that the small Cu clusters being formed initially can be observed by EXAFS, while they are still too small to be observed with XRD. This result is in good agreement with the conclusions of the study in ref. [2]. The results displayed in fig. 6 confirm that the reduction is completed within ca. 4 K under the present conditions. The fact that the curves smoothly change from one level to another without any additional features suggests that apparently no intermediate phases, like Cu<sub>2</sub>O, are formed in measurable amounts during reduction. Therefore, the results of the combined XRD/EXAFS study indicate that the



transformation of CuO to metallic Cu occurs directly or alternatively the relative concentration of an intermediate phase is so low that it escapes detection. This would be the case if, for example, the reduction of Cu<sub>2</sub>O to metallic Cu is much faster than the reduction of CuO to Cu<sub>2</sub>O. Studies are presently being performed to obtain further insight into the reduction process.

#### 4.2. VERIFICATION OF THE IMPROVED EXAFS ANALYSIS FOR SMALL PARTICLES

One of the major advantages of the application of EXAFS to the study of catalysts is its ability to provide in situ structural information on X-ray amorphous phases. Furthermore, the technique is capable of determining structural parameters, like bond lengths and coordination numbers. Since an accurate determination of the coordination number is the basis for a reliable estimation of the particle sizes by EXAFS, systematic errors in the coordination number analysis will result in large errors in the average particle sizes reported. We have recently shown [7,8] that the commonly used EXAFS analysis procedures may introduce large errors in the determination of the coordination numbers. An improved procedure was suggested based on molecular dynamics simulations and presently we will use the unique features of the combined EXAFS/XRD setup to verify experimentally the advantages of the new procedure.

The limitations of the standard EXAFS analysis are related to the fact that the atomic motion in small particles is very anharmonic [21]. This anharmonicity may introduce significant errors in the apparent bond distance [21] when determined by use of the standard EXAFS analysis which assumes that the thermal vibrations are harmonic (see, e.g., ref. [22]). In the present context, it is even more important that also the apparent EXAFS coordination numbers will be strongly influenced by the anharmonicity if the standard analysis is used for treating data of systems with small particles [7,8]. The fact that the motion of the atoms in small particles is very anharmonic, especially at high temperature, gives rise to asymmetric pair distribution functions with broad tails that contribute to the low  $k$  part of the EXAFS spectrum. This has important consequences for the analysis of experimentally measured X-ray absorption spectra since the near edge structure (corresponding to the small  $k$  part up to about  $3 \text{ \AA}^{-1}$ ) is dominated by multiple scattering effects and life time broadening of the final state and this region is, therefore, normally not included in the EXAFS analysis. The absence of low momentum transfer information and the non-transferability of amplitude functions between the reference bulk material and the small particles have the effect that the obtained coordination numbers are systematically too small. The errors introduced by these effects have been estimated by performing the standard analysis on EXAFS spectra derived from molecular dynamics simulations where the whole  $k$ -region is available [7,8]. The calculations were carried out for Cu particles with different diameters and at different temperatures. On the basis of this new procedure for correcting the apparent coordination numbers, it is possible to construct a relationship between

the apparent EXAFS coordination number and the particle size (see fig. 7 and refs. [7,8]).

In order to experimentally verify this new procedure, we have investigated silica supported Cu particles which are large enough to be observed by XRD but still so small that a significant reduction in the EXAFS coordination numbers can be observed. In this way one can use the combined EXAFS/XRD setup to record simultaneous XRD and EXAFS data on the *same* sample under *identical* conditions, thus ensuring that the two sets of data indeed result from identical catalyst structures. Quantitative XRD studies were carried out separately on physical mixtures of metallic Cu and SiO<sub>2</sub> to verify that all the Cu is observed by the XRD and that large amounts of Cu particles being below the critical size necessary for obtaining an XRD diffractogram are not present.

The EXAFS spectra showed the presence of small metallic Cu particles as evi-

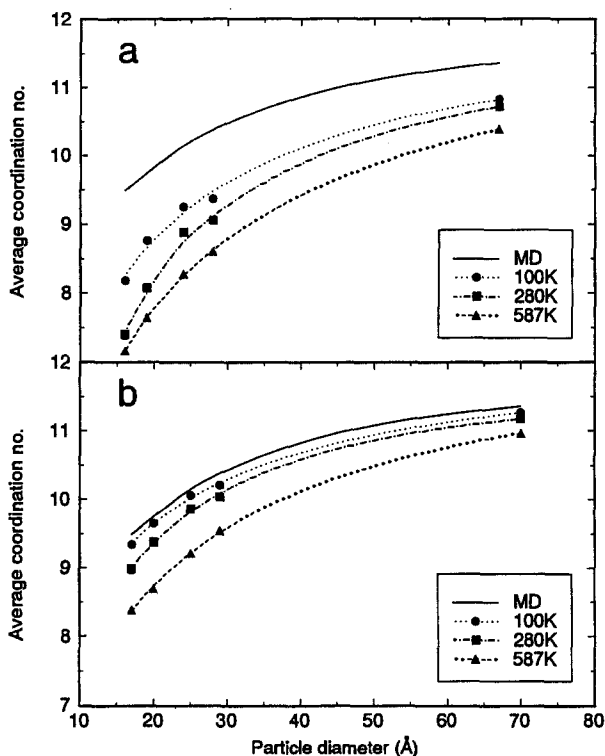


Fig. 7. Relation between the average coordination number and the Cu particle size. The curve denoted MD shows the relationship between true coordination numbers and particle size. The equilibrium configuration of the particles from the molecular dynamics simulations are used to establish this relationship [7]. The curves at the three different temperatures are obtained for the same particles and show the apparent coordination numbers using the standard EXAFS analysis ( $k^1$ -weighting and curve-fitting from 3–20 Å<sup>-1</sup>). (a) Debye–Waller factor constrained to be equal to that of bulk Cu.

(b) Debye–Waller factor treated as an adjustable parameter.

denced from the reduced peak amplitudes in the Fourier transforms [7]. The results of the standard EXAFS analysis for the 10% Cu/SiO<sub>2</sub> catalysts at 300 and 493 K reveal the apparent coordination numbers listed in table 1. In one analysis the Debye–Waller factor has been constrained to be identical to that of bulk Cu at the same temperature ( $\Delta\sigma^2 = 0$ ). Intuitively, one would find this to be a reasonable assumption of the atoms in the small particles move in a harmonic potential identical to that of the bulk. In another analysis the Debye–Waller factor was treated as an adjustable parameter. This results in somewhat higher apparent coordination numbers indicating that the disorder or the thermal vibrations of the atoms are larger in the small particles than in the bulk. The mean particle sizes corresponding to the apparent coordination numbers from the two analyses are between 10 and 17 Å (table 1). X-ray diffractograms of the Cu(111) diffraction line for the 10% Cu/SiO<sub>2</sub> catalyst at the two temperatures are shown in fig. 8. From a line profile analysis, an average XRD crystallite size of 30–35 Å (table 1) is estimated using the Debye–Scherrer formula with the Scherrer constant equal to 0.9. Thus, regardless of the analysis used, the standard EXAFS analysis gives systematically smaller particle sizes compared to the XRD technique. The difference in values obtained by the two techniques has been visualized in fig. 8. In addition to the experimentally obtained XRD diagrams we have plotted (with dashed line) the hypothetical diagrams corresponding to the particle size estimated from the standard EXAFS analysis with the Debye–Waller factor as an adjustable parameter. The disagreement is even larger if the Debye–Waller factor was constrained to be equal to that of the bulk.

The discrepancy in particle sizes can be quantitatively accounted for by applying the new procedure (fig. 7) for correcting the EXAFS coordination numbers obtained from the standard analysis. The XRD diagram corresponding to the corrected EXAFS particle sizes (solid line in fig. 8) is in good agreement with the experimentally obtained XRD results (see also table 1). Thus, fig. 7 can be used to correct the coordination numbers obtained from the standard EXAFS analysis procedure. It should be kept in mind, however, that quantitatively this figure is

Table 1

Apparent coordination numbers, relative Debye–Waller factors, and mean particle diameters for the reduced 10% Cu/SiO<sub>2</sub> catalyst

Temperature (K)	App. coord. number	$\Delta\sigma^2$ ( $\times 10^3$ )	$D$ (Å)		
			std. method	XRD <sup>a</sup>	new meth.
300	9.0	0	11.5	35	28
493	8.5 <sup>b</sup>	0	10.5	30	25
300	10.2	1.48	17.0	35	31
493	9.3 <sup>b</sup>	1.20	12.0	30	24

<sup>a</sup> Uncertainties of the XRD results are about  $\pm 5$  Å.

<sup>b</sup> Reference (bulk Cu metal) also measured at 493 K.

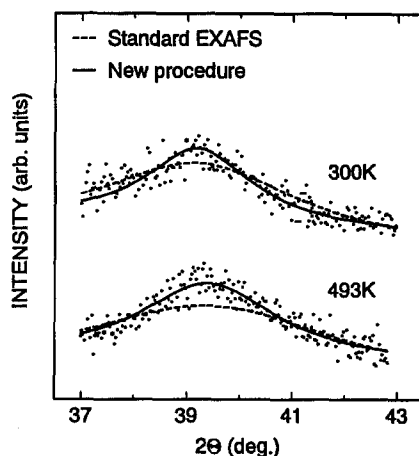


Fig. 8. X-ray diffractograms showing the Cu(111) line in the 10% Cu/SiO<sub>2</sub> catalyst at 300 and 493 K acquired using the combined XRD/EXAFS setup. The dashed line shows the calculated broadening of the Cu(111) peak corresponding to particles with the mean size determined by use of the standard EXAFS analysis and with the Debye–Waller factor as an adjustable parameter. The full line shows the results when the new procedure is used to estimate the Cu particle size.

valid for Cu only. Qualitatively, similar phenomena will also be present in other metals and studies are now in progress to extend the work [23].

## 5. Conclusion

A new combined QEXAFS/XRD method has been developed allowing both EXAFS and XRD experiments in the transmission mode to be carried out on the *same* sample under *identical* catalytic conditions. The major advantages of the setup can be summarized as follows:

- The use of the capillary microreactor/*in situ* cell allows realistic catalytic and structural information to be obtained simultaneously such that structure–activity relationships can be established.
- The possibility to obtain information on both crystalline and X-ray amorphous phases enables a more complete structural description of catalytic materials.
- The combined QEXAFS/XRD method allows high quality data to be recorded enabling quantitative analysis.
- The high degree of temperature uniformity of the reaction cell and the very fast response time of the system make dynamic studies feasible such that reliable information on phase transformations occurring within a few kelvin can be obtained.

These unique features of the combined method have been used to perform time resolved studies on the time scale of a few minutes of Cu-based methanol catalysts. These studies have provided important information on the possible presence of intermediate phases during the calcination and reduction processes. Furthermore, the combined EXAFS/XRD method has been used to confirm the advantages of a new procedure for obtaining a better estimation of the coordination numbers for small metallic particles from EXAFS.

## Acknowledgement

The authors are grateful to HASYLAB for offering beam time at the RÖMO II beamline and to the Danish Research Councils for financial support through the Center for Surface Reactivity. R. Frahm is gratefully acknowledged for making available to us the QEXAFS setup and for many helpful discussions on the application of QEXAFS.

## References

- [1] R. Prins and D.C. Koningsberger, in: *X-ray Absorption: Principles, Applications, Techniques of EXAFS, SEXAFS and XANES*, eds. D.C. Koningsberger and R. Prins (Wiley, New York, 1988) p. 321.
- [2] B.S. Clausen, G. Steffensen, B. Fabius, J. Villadsen, R. Feidenhans'l and H. Topsøe, *J. Catal.* 132 (1991) 524.
- [3] B.S. Clausen, L. Gråbæk, G. Steffensen and H. Topsøe, *HASYLAB Annual Report* (1991) p. 495;  
B.S. Clausen, L. Gråbæk, G. Steffensen, P.L. Hansen and H. Topsøe, *HASYLAB Annual Report* (1992) p. 223.
- [4] J.W. Couves, J.M. Thomas, D. Waller, T.H. Jones, A.J. Dent, G.E. Derbyshire and G.N. Greaves, *Nature* 354 (1991) 465.
- [5] A.J. Dent, M.P. Wells, R.C. Farrow, C.A. Ramsdale, G.E. Derbyshire, G.N. Greaves, J.W. Couves and J.M. Thomas, *Rev. Sci. Instr.* 63 (1992) 903.
- [6] R. Frahm, *Nucl. Instr. Meth. Phys. Res. A* 270 (1988) 578.
- [7] B.S. Clausen, L. Gråbæk, H. Topsøe, L.B. Hansen, P. Stoltze, J.K. Nørskov and O.H. Nielsen, *J. Catal.* 140 (1993), in press.
- [8] B.S. Clausen, H. Topsøe, L.B. Hansen, P. Stoltze and J.K. Nørskov, *Japan. Appl. Phys.*, in press.
- [9] B.S. Rasmussen, P.E. Højlund Nielsen, J. Villadsen and J.B. Hansen, in: *Preparation of Catalysts*, Vol. 4, eds. B. Delmon, P. Grange, P.A. Jacobs and G. Poncelet (Elsevier, Amsterdam, 1987) p. 785.
- [10] J.A. van Dillen, J.W. Geus, L.A.M. Hermans and J. van der Meijden, in: *Proc. 6th Int. Congr. on Catalysis*, eds. G.C. Bond, P.E. Wells and F.C. Tompkins (The Chemical Society, London, 1976) p. 677.
- [11] K. Klier, *Appl. Surf. Sci.* 19 (1984) 267.
- [12] G.C. Chinchin, K.C. Waugh and D.A. Whan, *Appl. Catal.* 25 (1986) 101.
- [13] R. Burch, S.E. Golunski and M.S. Spencer, *Catal. Lett.* 5 (1990) 55.

- [14] K. Shimomura, K. Ogawa, M. Oba and Y. Kotera, *J. Catal.* 52 (1978) 191.
- [15] K. Tohji, Y. Udagawa, T. Mizushima and A. Ueno, *J. Phys. Chem.* 89 (1985) 5671.
- [16] B.S. Clausen, B. Lengeler, B.S. Rasmussen, W. Niemann and H. Topsøe, *J. Phys. (Paris) C8* (1986) 237.
- [17] T.L. Neils and J.M. Burlitch, *J. Catal.* 118 (1989) 79.
- [18] D. Duprez, Z. Fer-Hamida and M.M. Bettahar, *J. Catal.* 124 (1990) 1.
- [19] B.S. Clausen and H. Topsøe, *Catal. Today* 9 (1991) 189.
- [20] G.D. Moggridge, T. Rayment, R.M. Ormerod, M.A. Morris and R.M. Lambert, *Nature* 358 (1992) 658.
- [21] L.B. Hansen, P. Stoltze, J.K. Nørskov, B.S. Clausen and W. Niemann, *Phys. Rev. Lett.* 64 (1990) 3155.
- [22] D.E. Sayers, E.A. Stern and F.W. Lytle, *Phys. Rev. Lett.* 27 (1971) 1204.
- [23] B.S. Clausen, H. Topsøe, L.B. Hansen, P. Stoltze and J.K. Nørskov, Paper to be presented at the National ACS Meeting, Chicago, Illinois, 22–27 August 1993.